Observation of $\psi(3686) \longrightarrow \Lambda\bar{\Lambda}\eta'$

BESIII Collaboration (not published), BAM-00421

汇报人：兰文宁

BUSINESS

目 录

研究背景

- 作为c和反c夸克的束缚态，charmonium（粲偶素）态与远程相互作用有关，这提供了有关非微扰QCD在重夸克有效理论不适用的低能量区中的信息。
- charmonium衰变中重子的高产生率。e+ e-湮灭产生J/ψ 和 ψ(3686) 衰变的大量数据样本，为研究激发重子提供了极好的机会。
- 基于用bes 3探测器收集的27亿个 ψ(3686) 事例，首次观察到了 ψ(3686) →ΛΛη'，并提供了一个寻找 Λ＊(Λ＊) 的机会，它由Λη′ (Λη′) 组成。

研究内容

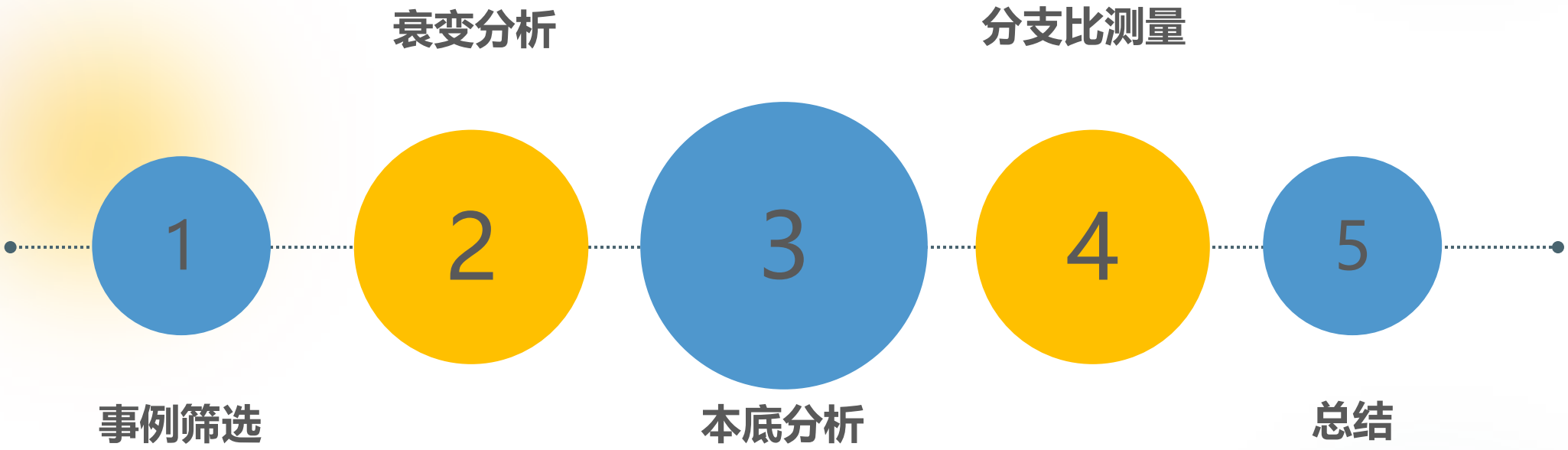

数据样本

BOSS version: 709

2.7×10^9 ψ(3686) events from data

2.7×10^9 ψ(3686) inclusive MC sample

2.6×10^6 ψ(3686) exclusive MC

center-of-mass energy for continuum backgrounds （连续本底）

3.65GeV/c2

3.682GeV/c2

研究内容

衰变分析

$\psi(3686) \to \Lambda \bar{\Lambda} \eta'$

$\eta' \to \gamma\pi^+\pi^-$ (mode 1)

$\eta' \to \eta\pi^+\pi^-$ (mode 2)

$\Lambda(\bar{\Lambda}) \to p\pi^-$ ($\bar{p}\pi^+$) ($\Lambda(\bar{\Lambda})$rec)

$\eta \to \gamma\gamma$

Mode 1

末态粒子为p π− $\bar{p}$ π+ π+π− γ

包括6条带电径迹, 1个γ光子

Mode 2

末态粒子为p π− $\bar{p}$ π+π+π−γγ

包括6条带电径迹2个γ光子

Table 1: Exclusive MC samples

Decay Mode	Generator	Number of events
$\psi(3686) \to \Lambda\bar{\Lambda}\eta', \eta' \to \gamma\pi^+\pi^-$	*PHSP, DIY_Etap2gpipi_box0*	2.6×10^6
$\psi(3686) \to \Lambda\bar{\Lambda}\eta', \eta' \to \eta\pi^+\pi^-, \eta \to \gamma\gamma$	*PHSP, DIY_pipieta*	2.6×10^6

研究内容

衰变分析（mode 1）

$\psi(3686) \rightarrow \Lambda\,\bar{\Lambda}\eta'$

$\eta' \rightarrow \gamma\pi^+\pi^-$

$\Lambda(\bar{\Lambda}) \rightarrow p\pi^-$ （ $\bar{p}\pi^+$ ） （$\Lambda(\bar{\Lambda})$rec)

事例筛选

Criteria	Efficiency(%)
$N_{charged} \geqslant 6$	42.59
Pass PID	30.01
$\Lambda\bar{\Lambda}$ reconstruction	29.06
$\pi^+\pi^-$ vertex fit	23.57
$N_\gamma \geqslant 1$	23.44
Pass 4C	15.14
$\chi^2_{4C} < 30$	10.35
$\lvert M_{p\pi^-(\bar{p}\pi^+)} - M_{\Lambda(\bar{\Lambda})}\rvert < 6$ MeV/c^2	9.23
$\lvert M_{\gamma\Lambda(\bar{\Lambda})} - M_{\Sigma^0(\bar{\Sigma}^0)}\rvert > 10$ MeV/c^2	8.81
$\lvert M^{\pi^+\pi^-}_{recoil} - M_{J/\psi}\rvert > 8$ MeV/c^2	8.77
veto χ_{cJ} mass region	6.83
veto $\Sigma(1385)$ and $\Xi^-(\bar{\Xi}^+)$ mass region	6.54

1

2

3

带电径迹selection

MDC中的极角必须满足 | Cos θ |<0.93

带电径迹的数量需要超过6条

PID selection

结合它们的TOF和dE/dx信息进行粒子鉴别 (PID)

(Prob(i)，i = π，K，p)，如果带电径迹在π或p 的假设下得到的Prob大于其他粒子假设下的Prob，则该带电径迹将被识别为π或p

Λ $\bar{\Lambda}$ Reconstruction

满足次级顶点约束

至少一个p π-(Λ) 和一个 $\bar{p}$ π+($\bar{\Lambda}$)

有多个 Λ Λ 时，选择一对 (Mpπ−− MΛ)2 + (Mpπ+ − $M_{\bar{\Lambda}}$)2最小的Λ $\bar{\Lambda}$

事例筛选

Criteria	Efficiency(%)
$N_{charged} \geqslant 6$	42.59
Pass PID	30.01
$\Lambda\bar{\Lambda}$ reconstruction	29.06
$\pi^+\pi^-$ vertex fit	23.57
$N_\gamma \geqslant 1$	23.44
Pass 4C	15.14
$\chi^2_{4C} < 30$	10.35
$\lvert M_{p\pi^-(\bar{p}\pi^+)} - M_{\Lambda(\bar{\Lambda})}\rvert < 6$ MeV/c^2	9.23
$\lvert M_{\gamma\Lambda(\bar{\Lambda})} - M_{\Sigma^0(\bar{\Sigma}^0)}\rvert > 10$ MeV/c^2	8.81
$\lvert M^{\pi^+\pi^-}_{recoil} - M_{J/\psi}\rvert > 8$ MeV/c^2	8.77
veto χ_{cJ} mass region	6.83
veto $\Sigma(1385)$ and $\Xi^-(\bar{\Xi}^+)$ mass region	6.54

4

5

6

π+π− Reconstructio

(| z | < 10cm

Xy面半径<1cm

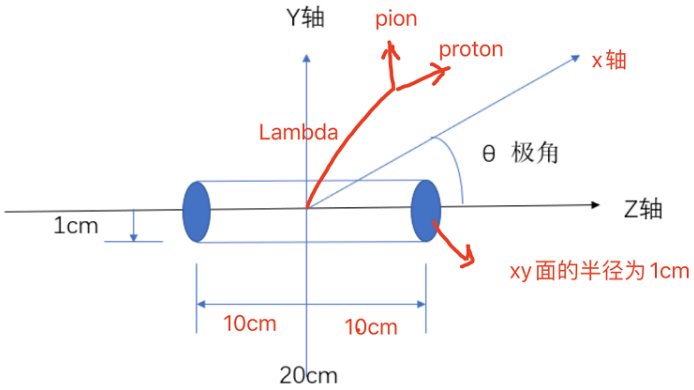

Good Photon Select

在桶身区域的最小能量25 MeV (| Cos θ | < 0.80)

在端盖区域的最小能量50 MeV (0.86<| cos θ |<0.92)

时间在[0，700] ns范围内

与最近的带电径迹至少间隔10 °

至少1个γ光子

Kinematic fit（运动学拟合）

对事例进行运动学拟合使之满足能量守恒三动量守恒

给带电径迹分配相应的的带电粒子

事例中有多个γ时，选择χ^2最小的组合

4C的χ^2

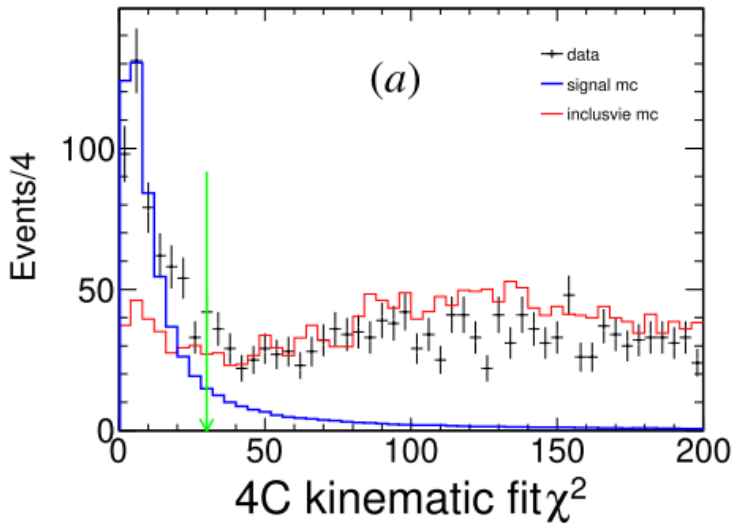

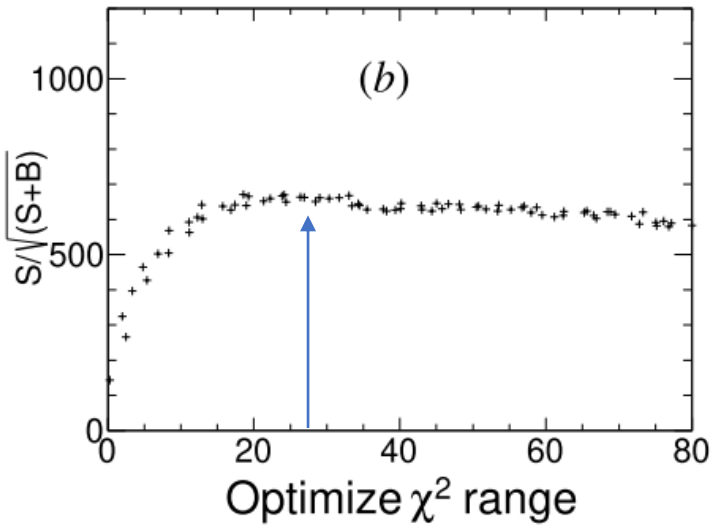

Criteria	Efficiency(%)
$N_{charged} \geqslant 6$	42.59
Pass PID	30.01
$\Lambda\bar{\Lambda}$ reconstruction	29.06
$\pi^+\pi^-$ vertex fit	23.57
$N_\gamma \geqslant 1$	23.44
Pass 4C	15.14
$\chi^2_{4C} < 30$	10.35
$\lvert M_{p\pi^-(\bar{p}\pi^+)} - M_{\Lambda(\bar{\Lambda})}\rvert < 6$ MeV/c^2	9.23
$\lvert M_{\gamma\Lambda(\bar{\Lambda})} - M_{\Sigma^0(\bar{\Sigma}^0)}\rvert > 10$ MeV/c^2	8.81
$\lvert M^{\pi^+\pi^-}_{recoil} - M_{J/\psi}\rvert > 8$ MeV/c^2	8.77
veto χ_{cJ} mass region	6.83
veto $\Sigma(1385)$ and $\Xi^-(\bar{\Xi}^+)$ mass region	6.54

Figure 1: The distribution 4C kinematic fit χ^2 (a) and the optimization result (b).

Λ($\bar{\Lambda}$)→ pπ−（$\bar{p}$π+）的不变质量谱

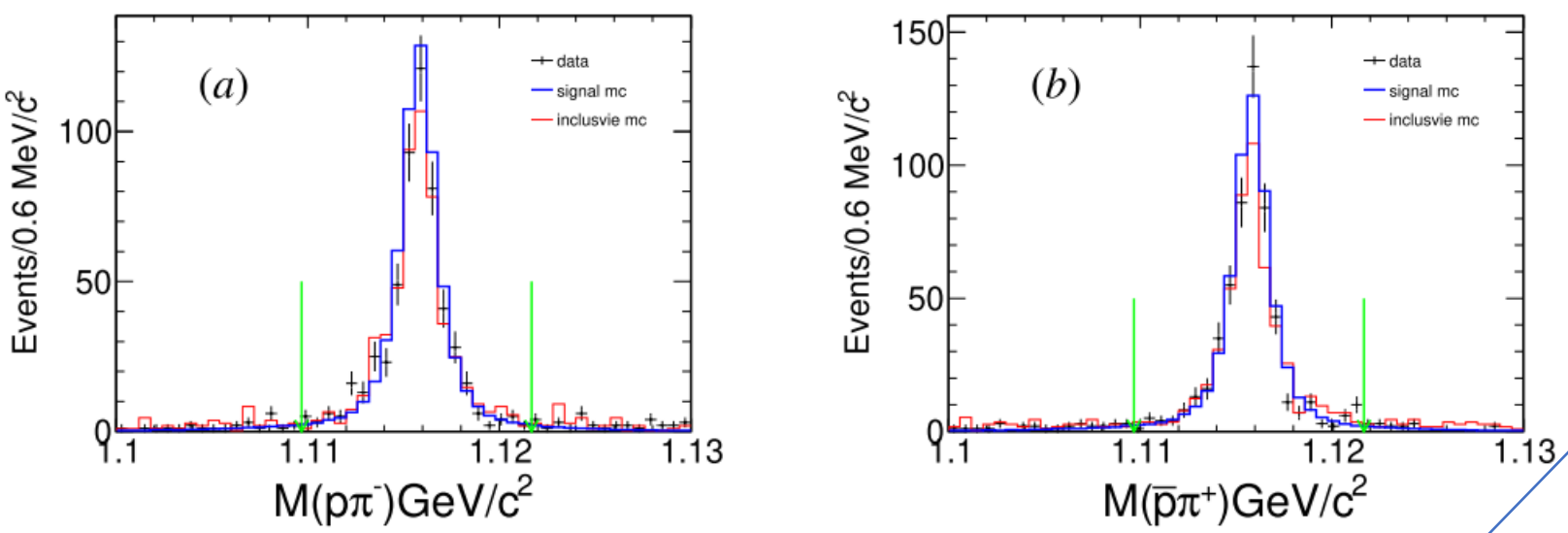

Criteria	Efficiency(%)
$N_{charged} \geqslant 6$	42.59
Pass PID	30.01
$\Lambda\bar{\Lambda}$ reconstruction	29.06
$\pi^+\pi^-$ vertex fit	23.57
$N_\gamma \geqslant 1$	23.44
Pass 4C	15.14
$\chi^2_{4C} < 30$	10.35
$\lvert M_{p\pi^-(\bar{p}\pi^+)} - M_{\Lambda(\bar{\Lambda})}\rvert < 6$ MeV/c^2	9.23
$\lvert M_{\gamma\Lambda(\bar{\Lambda})} - M_{\Sigma^0(\bar{\Sigma}^0)}\rvert > 10$ MeV/c^2	8.81
$\lvert M^{\pi^+\pi^-}_{recoil} - M_{J/\psi}\rvert > 8$ MeV/c^2	8.77
veto χ_{cJ} mass region	6.83
veto $\Sigma(1385)$ and $\Xi^-(\bar{\Xi}^+)$ mass region	6.54

Figure 2: The invariant mass distributions of $p\pi^-$ (a) and $\bar{p}\pi^+$ (b).

本底分析

去除 Sigma^0 的本底

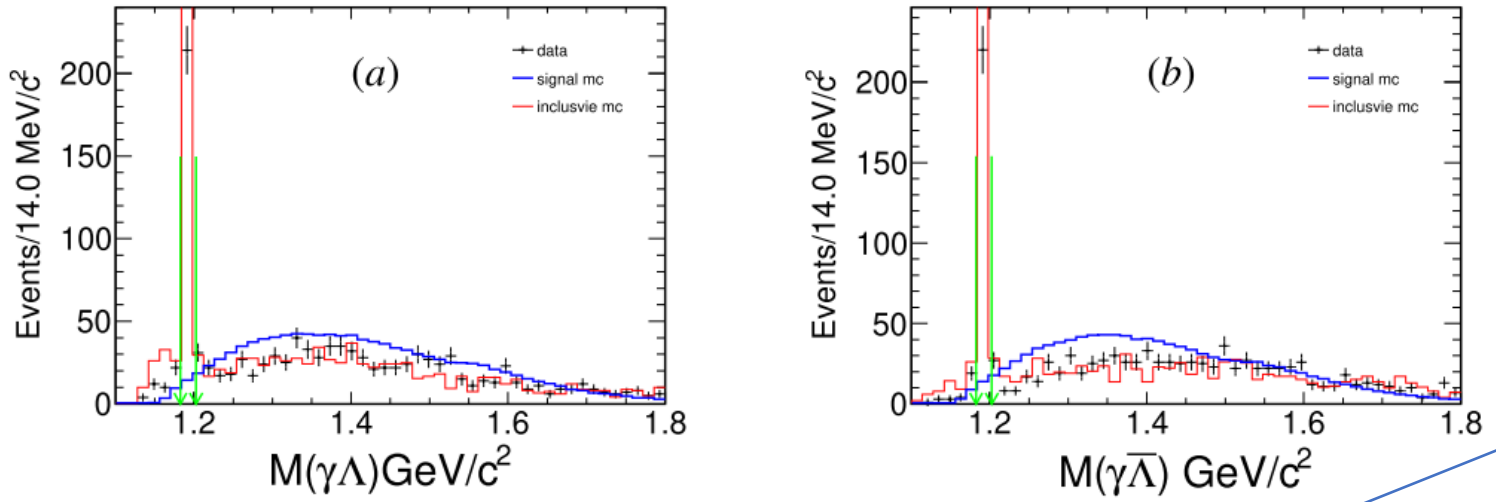

Figure 3: The mass distribution of $\gamma\Lambda$ and $\gamma\bar{\Lambda}$.

Criteria	Efficiency(%)
$N_{charged} \geqslant 6$	42.59
Pass PID	30.01
$\Lambda\bar{\Lambda}$ reconstruction	29.06
$\pi^+\pi^-$ vertex fit	23.57
$N_\gamma \geqslant 1$	23.44
Pass 4C	15.14
$\chi^2_{4C} < 30$	10.35
$\lvert M_{p\pi^-(\bar{p}\pi^+)} - M_{\Lambda(\bar{\Lambda})}\rvert < 6$ MeV/c^2	9.23
$\lvert M_{\gamma\Lambda(\bar{\Lambda})} - M_{\Sigma^0(\bar{\Sigma}^0)}\rvert > 10$ MeV/c^2	8.81
$\lvert M^{\pi^+\pi^-}_{recoil} - M_{J/\psi}\rvert > 8$ MeV/c^2	8.77
veto χ_{cJ} mass region	6.83
veto $\Sigma(1385)$ and $\Xi^-(\bar{\Xi}^+)$ mass region	6.54

去除psi(3686) -> pi+ pi- J/psi的本底

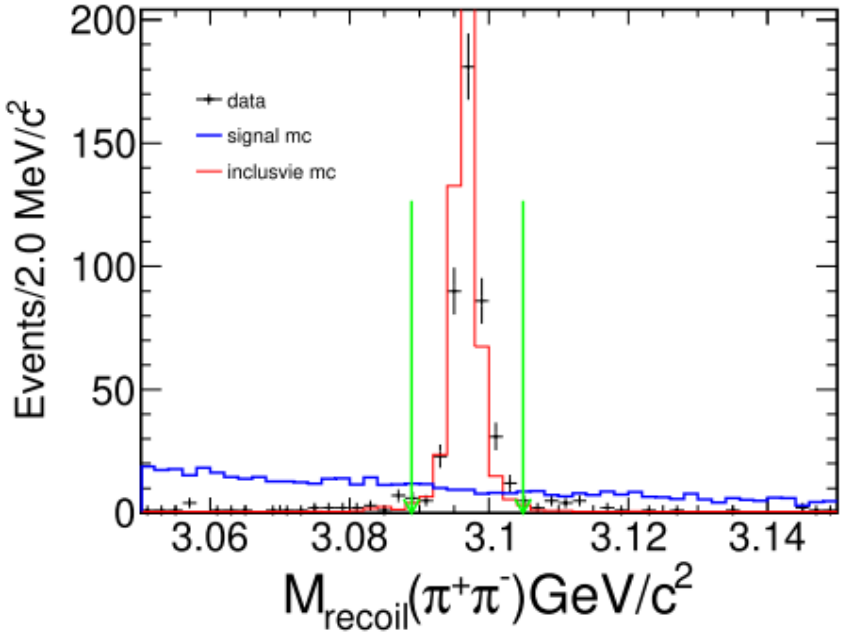

Figure 4: The invariant mass recoiling against the $\pi^+\pi^-$.

Criteria	Efficiency(%)
$N_{charged} \geqslant 6$	42.59
Pass PID	30.01
$\Lambda\bar{\Lambda}$ reconstruction	29.06
$\pi^+\pi^-$ vertex fit	23.57
$N_\gamma \geqslant 1$	23.44
Pass 4C	15.14
$\chi^2_{4C} < 30$	10.35
$\lvert M_{p\pi^-(\bar{p}\pi^+)} - M_{\Lambda(\bar{\Lambda})}\rvert < 6$ MeV/c^2	9.23
$\lvert M_{\gamma\Lambda(\bar{\Lambda})} - M_{\Sigma^0(\bar{\Sigma}^0)}\rvert > 10$ MeV/c^2	8.81
$\lvert M^{\pi^+\pi^-}_{recoil} - M_{J/\psi}\rvert > 8$ MeV/c^2	8.77
veto χ_{cJ} mass region	6.83
veto $\Sigma(1385)$ and $\Xi^-(\bar{\Xi}^+)$ mass region	6.54

去除psi(3686) -> gamma chi_cJ 的本底

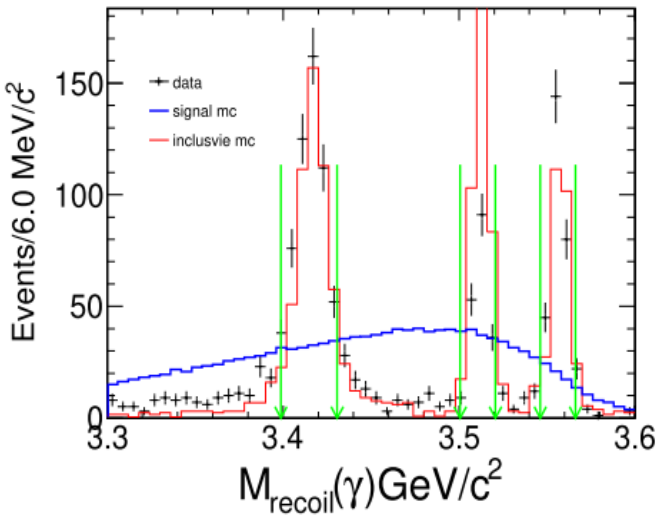

Figure 5: The distribution of invariant mass recoiling against the radiative photon.

Criteria	Efficiency(%)
$N_{charged} \geqslant 6$	42.59
Pass PID	30.01
$\Lambda\bar{\Lambda}$ reconstruction	29.06
$\pi^+\pi^-$ vertex fit	23.57
$N_\gamma \geqslant 1$	23.44
Pass 4C	15.14
$\chi^2_{4C} < 30$	10.35
$\lvert M_{p\pi^-(\bar{p}\pi^+)} - M_{\Lambda(\bar{\Lambda})}\rvert < 6$ MeV/c^2	9.23
$\lvert M_{\gamma\Lambda(\bar{\Lambda})} - M_{\Sigma^0(\bar{\Sigma}^0)}\rvert > 10$ MeV/c^2	8.81
$\lvert M^{\pi^+\pi^-}_{recoil} - M_{J/\psi}\rvert > 8$ MeV/c^2	8.77
veto χ_{cJ} mass region	6.83
veto $\Sigma(1385)$ and $\Xi^-(\bar{\Xi}^+)$ mass region	6.54

去除Sigma(1385)，Xi^-的本底

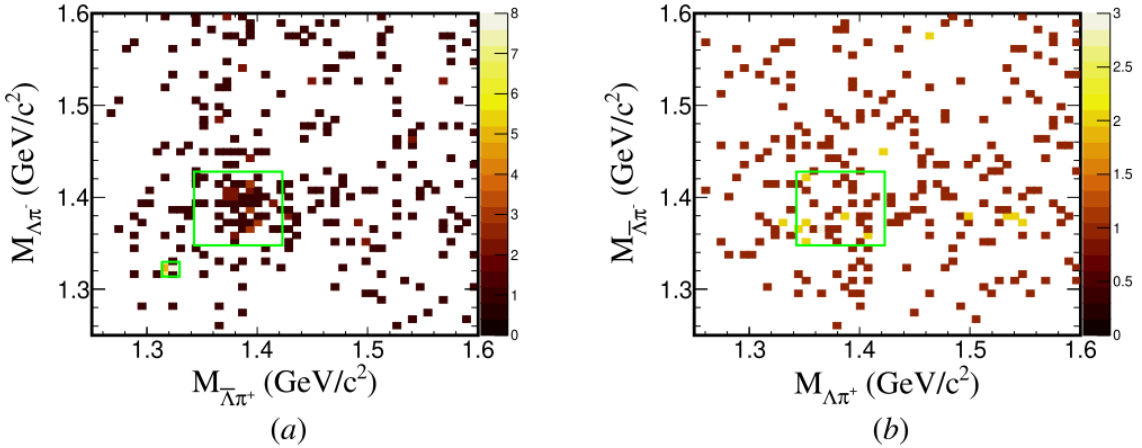

(a) (b)

Figure 6: The scatter plots of $\Lambda\pi^-$ versus $\bar{\Lambda}\pi^+$ (a) and $\bar{\Lambda}\pi^-$ versus $\Lambda\pi^+$ (b). The small box shown in (a) is the scatter plots of Ξ^- versus $\bar{\Xi}^+$, and the mass window determined to be 8 MeV/c^2. And the mass window of the two big boxes which indicated Σ^{*-} versus $\bar{\Sigma}^{*+}$(+ c.c) are 40 MeV/c^2.

Criteria	Efficiency(%)
$N_{charged} \geqslant 6$	42.59
Pass PID	30.01
$\Lambda\bar{\Lambda}$ reconstruction	29.06
$\pi^+\pi^-$ vertex fit	23.57
$N_\gamma \geqslant 1$	23.44
Pass 4C	15.14
$\chi^2_{4C} < 30$	10.35
$\lvert M_{p\pi^-(\bar{p}\pi^+)} - M_{\Lambda(\bar{\Lambda})}\rvert < 6$ MeV/c^2	9.23
$\lvert M_{\gamma\Lambda(\bar{\Lambda})} - M_{\Sigma^0(\bar{\Sigma}^0)}\rvert > 10$ MeV/c^2	8.81
$\lvert M^{\pi^+\pi^-}_{recoil} - M_{J/\psi}\rvert > 8$ MeV/c^2	8.77
veto χ_{cJ} mass region	6.83
veto $\Sigma(1385)$ and $\Xi^-(\bar{\Xi}^+)$ mass region	6.54

Eta’ -> gamma pi+ pi- 的选择

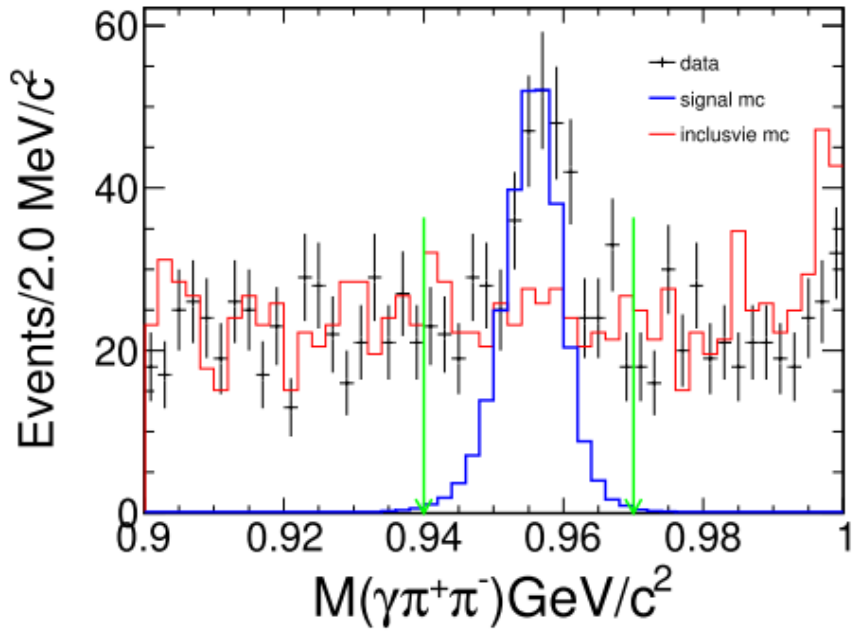

Figure 7: The invariant mass distribution of $\gamma\pi^+\pi^-$

Criteria	Efficiency(%)
$N_{charged} \geqslant 6$	42.59
Pass PID	30.01
$\Lambda\bar{\Lambda}$ reconstruction	29.06
$\pi^+\pi^-$ vertex fit	23.57
$N_\gamma \geqslant 1$	23.44
Pass 4C	15.14
$\chi^2_{4C} < 30$	10.35
$\lvert M_{p\pi^-(\bar{p}\pi^+)} - M_{\Lambda(\bar{\Lambda})}\rvert < 6$ MeV/c^2	9.23
$\lvert M_{\gamma\Lambda(\bar{\Lambda})} - M_{\Sigma^0(\bar{\Sigma}^0)}\rvert > 10$ MeV/c^2	8.81
$\lvert M^{\pi^+\pi^-}_{recoil} - M_{J/\psi}\rvert > 8$ MeV/c^2	8.77
veto χ_{cJ} mass region	6.83
veto $\Sigma(1385)$ and $\Xi^-(\bar{\Xi}^+)$ mass region	6.54

通过事例筛选之后的topology分析

Table 3: The dominant background contributions to $\psi(3686) \to \Lambda\bar{\Lambda}\eta', \eta' \to \gamma\pi^+\pi^-$.

No.	Decay tree	iDcyTr	Number of events
1	$\psi(3686) \to \pi^+\pi^- J/\psi, J/\psi \to \Lambda\bar{\Lambda}\gamma, \Lambda \to \pi^- p, \bar{\Lambda} \to \pi^+\bar{p}$	1	159
2	$\psi(3686) \to \chi_{c0}\gamma, \chi_{c0} \to \pi^+\Lambda\bar{\Sigma}^{*-}, \Lambda \to \pi^- p, \bar{\Sigma}^{*-} \to \pi^-\bar{\Lambda}, \bar{\Lambda} \to \pi^+\bar{p}$	0	38
3	$\psi(3686) \to \chi_{c0}\gamma, \chi_{c0} \to \pi^+\Sigma^{*-}\bar{\Lambda}, \Sigma^{*-} \to \pi^-\Lambda, \bar{\Lambda} \to \pi^+\bar{p}, \Lambda \to \pi^- p$	3	29
4	$\psi(3686) \to \chi_{c0}\gamma, \chi_{c0} \to \pi^-\bar{\Lambda}\Sigma^{*+}, \bar{\Lambda} \to \pi^+\bar{p}, \Sigma^{*+} \to \pi^+\Lambda, \Lambda \to \pi^- p$	10	29
5	$\psi(3686) \to \chi_{c0}\gamma, \chi_{c0} \to \pi^-\bar{\Sigma}^{*+}\Lambda, \bar{\Sigma}^{*+} \to \pi^+\bar{\Lambda}, \Lambda \to \pi^- p, \bar{\Lambda} \to \pi^+\bar{p}$	14	29
6	$\psi(3686) \to \chi_{c2}\gamma, \chi_{c2} \to \pi^-\bar{\Lambda}\Sigma^{*+}, \bar{\Lambda} \to \pi^+\bar{p}, \Sigma^{*+} \to \pi^+\Lambda, \Lambda \to \pi^- p$	36	13
7	$\psi(3686) \to \chi_{c0}\gamma, \chi_{c0} \to K^{*+}\bar{p}\Lambda, K^{*+} \to \pi^+ K^0, \Lambda \to \pi^- p, K^0 \to K_S^0, K_S^0 \to \pi^+\pi^-$	48	13
8	$\psi(3686) \to \chi_{c2}\gamma, \chi_{c2} \to \pi^-\bar{\Sigma}^{*+}\Lambda, \bar{\Sigma}^{*+} \to \pi^+\bar{\Lambda}, \Lambda \to \pi^- p, \bar{\Lambda} \to \pi^+\bar{p}$	25	10
9	$\psi(3686) \to \chi_{c0}\gamma, \chi_{c0} \to K^{*-}p\bar{\Lambda}, K^{*-} \to \pi^-\bar{K}^0, \bar{\Lambda} \to \pi^+\bar{p}, \bar{K}^0 \to K_S^0, K_S^0 \to \pi^+\pi^-$	39	10
10	$\psi(3686) \to \chi_{c1}\gamma, \chi_{c1} \to \pi^-\bar{\Lambda}\Sigma^{*+}, \bar{\Lambda} \to \pi^+\bar{p}, \Sigma^{*+} \to \pi^+\Lambda, \Lambda \to \pi^- p$	26	10
11	$\psi(3686) \to \pi^-\bar{\Sigma}^{*+}\Lambda\gamma^f, \bar{\Sigma}^{*+} \to \pi^+\bar{\Lambda}, \Lambda \to \pi^- p, \bar{\Lambda} \to \pi^+\bar{p}$	50	10
12	$\psi(3686) \to \chi_{c2}\gamma, \chi_{c2} \to \pi^+\Lambda\bar{\Sigma}^{*-}, \Lambda \to \pi^- p, \bar{\Sigma}^{*-} \to \pi^-\bar{\Lambda}, \bar{\Lambda} \to \pi^+\bar{p}$	7	9
13	$\psi(3686) \to \chi_{c1}\gamma, \chi_{c1} \to \pi^+\Lambda\bar{\Sigma}^{*-}, \Lambda \to \pi^- p, \bar{\Sigma}^{*-} \to \pi^-\bar{\Lambda}, \bar{\Lambda} \to \pi^+\bar{p}$	11	8
14	$\psi(3686) \to \chi_{c1}\gamma, \chi_{c1} \to \pi^-\bar{\Sigma}^{*+}\Lambda, \bar{\Sigma}^{*+} \to \pi^+\bar{\Lambda}, \Lambda \to \pi^- p, \bar{\Lambda} \to \pi^+\bar{p}$	13	8
15	$\psi(3686) \to \chi_{c2}\gamma, \chi_{c2} \to \rho^0\Lambda\bar{\Lambda}, \rho^0 \to \pi^+\pi^-, \Lambda \to \pi^- p, \bar{\Lambda} \to \pi^+\bar{p}$	27	7
16	$\psi(3686) \to \pi^+\Lambda\bar{\Sigma}^{*-}\gamma^f, \Lambda \to \pi^- p, \bar{\Sigma}^{*-} \to \pi^-\bar{\Lambda}, \bar{\Lambda} \to \pi^+\bar{p}$	35	7
17	$\psi(3686) \to \pi^-\bar{\Lambda}\Sigma^{*+}, \bar{\Lambda} \to \pi^+\bar{p}, \Sigma^{*+} \to \pi^+\Lambda, \Lambda \to \pi^- p$	21	6
18	$\psi(3686) \to \eta'\Delta^{++}\bar{\Delta}^{--}, \eta' \to \pi^+\pi^-\gamma^F, \Delta^{++} \to \pi^+ p, \bar{\Delta}^{--} \to \pi^-\bar{p}$	43	1
others	Including 91 decay channels		175

连续本底的分析
e+ e-直接衰变到Lambda anti-Lambda eta’，中间没有psi(3686)

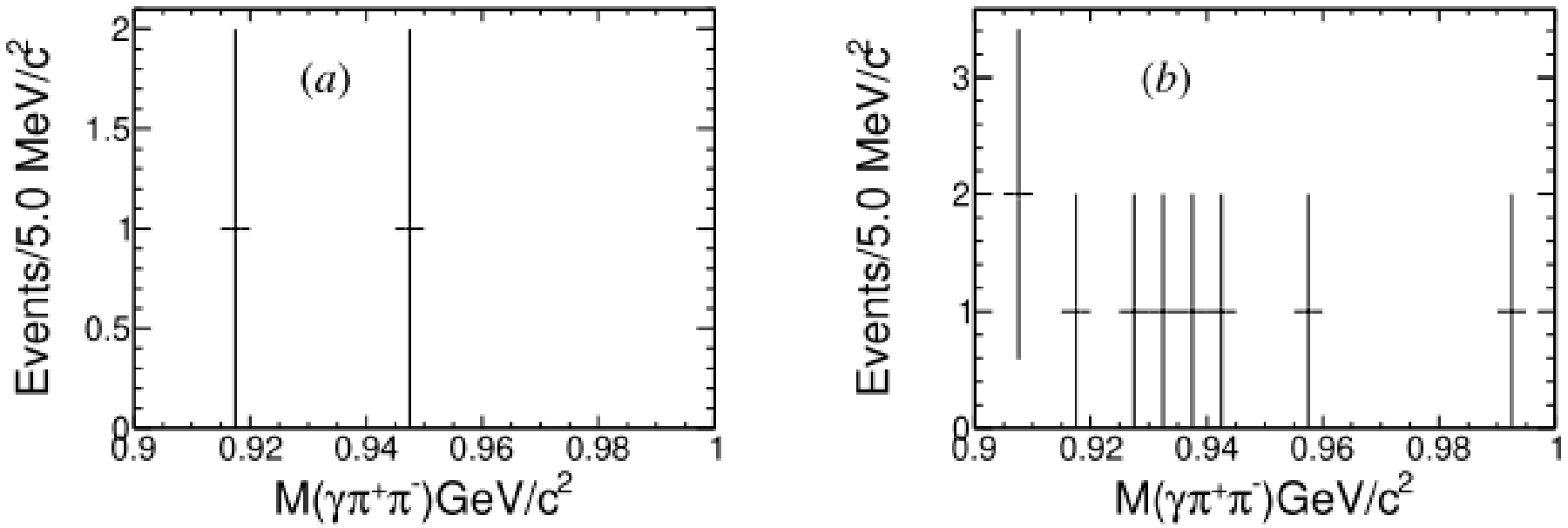

Figure 8: Invariant mass distributions of $\gamma\pi^+\pi^-$ at center-of-mass energy of 3.65 GeV/c^2 (a) and 3.682 GeV/c^2 (b).

研究内容

衰变分析（mode 2）

$\psi(3686) \rightarrow \Lambda\,\bar{\Lambda}\eta'$

$\eta' \rightarrow \eta\pi^+\pi^-$

$\Lambda(\bar{\Lambda}) \rightarrow p\pi^-$ （ $\bar{p}\pi^+$ ） （$\Lambda(\bar{\Lambda})$rec)

$\eta \rightarrow \gamma\gamma$

5C的χ^2分布

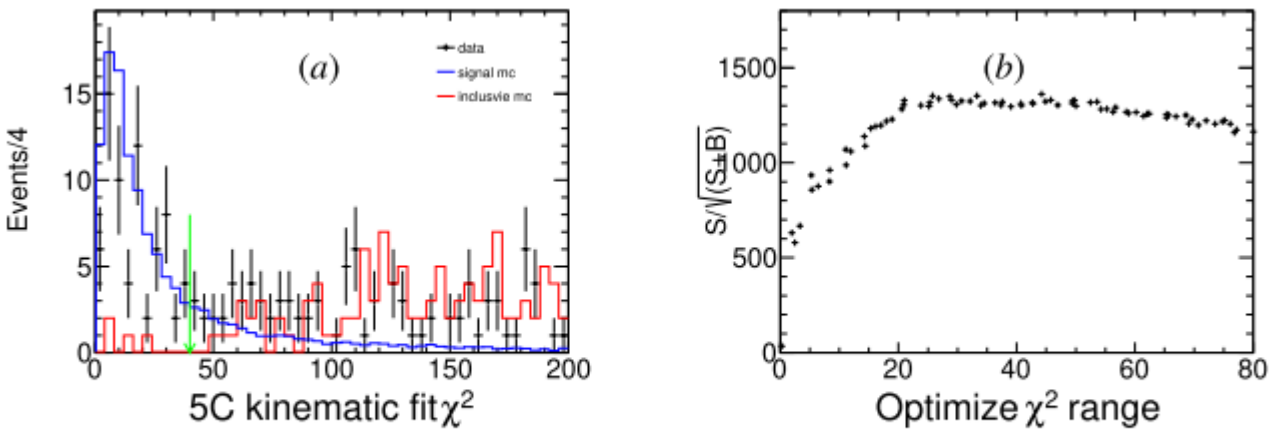

Figure 9: The distribution of 5C kinematic fit χ^2 (a) and the optimization result (b).

Criteria	Efficiency(%)
$N_{charged} \geqslant 6$	36.05
Pass PID	23.93
$\Lambda\bar{\Lambda}$ reconstruction	23.11
$\pi^+\pi^-$ vertex fit	15.86
$N_\gamma \geqslant 2$	15.41
Pass 5C	8.24
$\chi^2_{5C} < 40$	5.56
$M_{p\pi^-(\bar{p}\pi^+)} \in (1.108, 1.123)$ GeV/c^2	5.09
$\lvert M^{\eta}_{recoil} - M_{J/\psi}\rvert > 10$ MeV/c^2	4.58

Eta’ -> eta pi+ pi-的选择

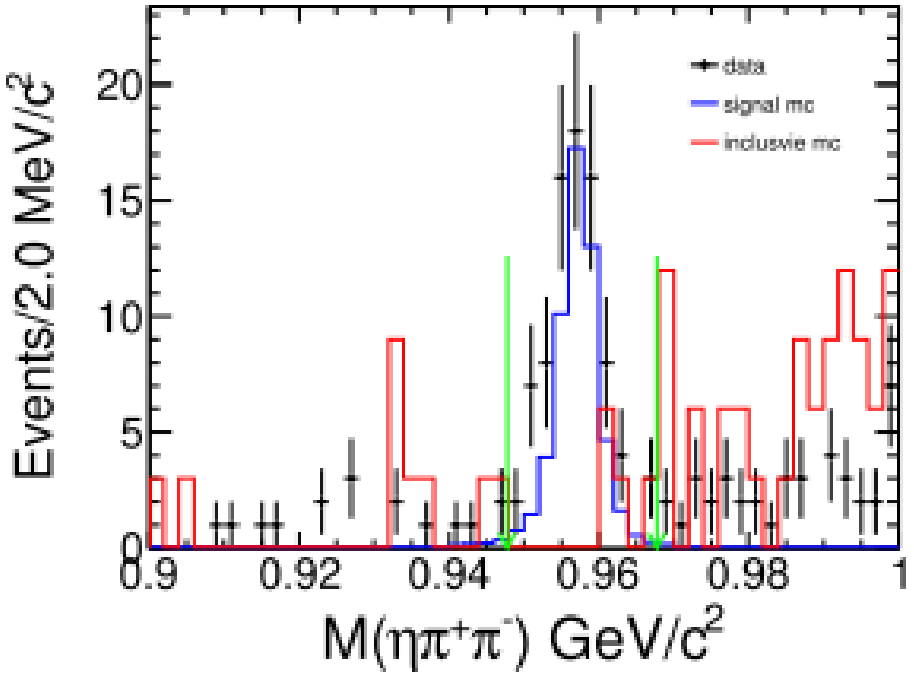

Criteria	Efficiency(%)
$N_{charged} \geqslant 6$	36.05
Pass PID	23.93
$\Lambda\bar{\Lambda}$ reconstruction	23.11
$\pi^+\pi^-$ vertex fit	15.86
$N_\gamma \geqslant 2$	15.41
Pass 5C	8.24
$\chi^2_{5C} < 40$	5.56
$M_{p\pi^-(\bar{p}\pi^+)} \in (1.108, 1.123)$ GeV/c^2	5.09
$\lvert M^{\eta}_{recoil} - M_{J/\psi}\rvert > 10$ MeV/c^2	4.58

Figure 10: The invariant mass distribution of $\eta\pi^+\pi^-$

$\Lambda(\bar{\Lambda})\rightarrow p\pi-$（$\bar{p}\pi+$）的不变质量谱

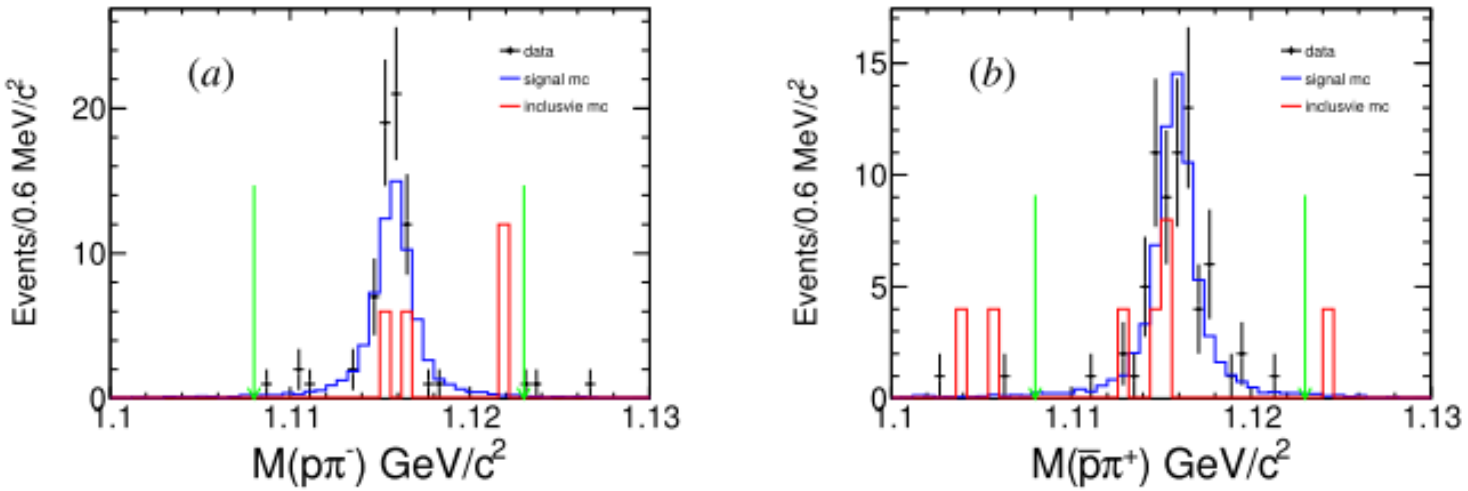

Figure 11: The invariant mass distribution of $p\pi^-$ (a) and $\bar{p}\pi^+$ (b)

Criteria	Efficiency(%)
$N_{charged} \geqslant 6$	36.05
Pass PID	23.93
$\Lambda\bar{\Lambda}$ reconstruction	23.11
$\pi^+\pi^-$ vertex fit	15.86
$N_\gamma \geqslant 2$	15.41
Pass 5C	8.24
$\chi^2_{5C} < 40$	5.56
$M_{p\pi^-(\bar{p}\pi^+)} \in (1.108, 1.123)$ GeV/c^2	5.09
$\lvert M^{\eta}_{recoil} - M_{J/\psi}\rvert > 10$ MeV/c^2	4.58

去除psi(3686) -> eta J/psi 的本底

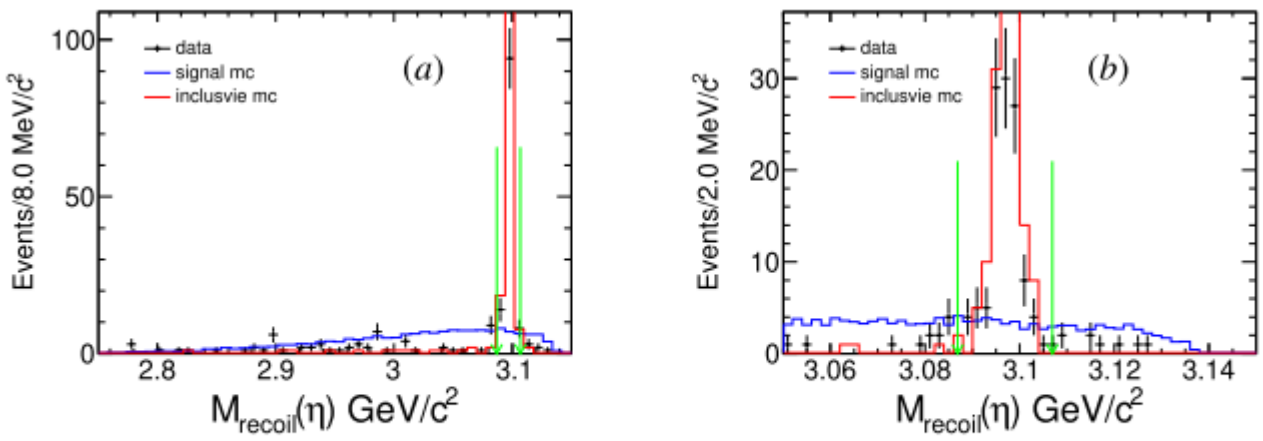

Criteria	Efficiency(%)
$N_{charged} \geqslant 6$	36.05
Pass PID	23.93
$\Lambda\bar{\Lambda}$ reconstruction	23.11
$\pi^+\pi^-$ vertex fit	15.86
$N_\gamma \geqslant 2$	15.41
Pass 5C	8.24
$\chi^2_{5C} < 40$	5.56
$M_{p\pi^-(\bar{p}\pi^+)} \in (1.108, 1.123)$ GeV/c^2	5.09
$\lvert M^{\eta}_{recoil} - M_{J/\psi}\rvert > 10$ MeV/c^2	4.58

Figure 12: The distribution of invariant mass recoiling against η (a) and the distribution in region (3.05,3.15) GeV/c^2 (b).

剩余事例的topology分析

Table 5: The dominant background contributions to $\psi(3686) \to \Lambda\bar{\Lambda}\eta', \eta' \to \eta\pi^+\pi^-$.

No.	Decay tree	iDcyTr	number of events
1	$\psi(3686) \to \pi^+\pi^- J/\psi, J/\psi \to \eta\Lambda\bar{\Lambda}, \eta \to \gamma\gamma, \Lambda \to \pi^- p, \bar{\Lambda} \to \pi^+\bar{p}$	7	8
2	$\psi(3686) \to \eta J/\psi, \eta \to \pi^0\pi^+\pi^-, J/\psi \to \Lambda\bar{\Lambda}\gamma, \Lambda \to \pi^- p, \bar{\Lambda} \to \pi^+\bar{p}$	6	5
3	$\psi(3686) \to \chi_{c1}\gamma, \chi_{c1} \to J/\psi\gamma, J/\psi \to \pi^+\pi^-\Lambda\bar{\Lambda}, \Lambda \to \pi^- p, \bar{\Lambda} \to \pi^+\bar{p}$	1	4
4	$\psi(3686) \to \eta\Sigma^{*+}\bar{\Sigma}^{*-}, \eta \to \gamma\gamma, \Sigma^{*+} \to \pi^+\Lambda, \bar{\Sigma}^{*-} \to \pi^-\bar{\Lambda}, \Lambda \to \pi^- p,$ $\bar{\Lambda} \to \pi^+\bar{p}$	2	4
5	$\psi(3686) \to \chi_{c0}\gamma, \chi_{c0} \to \pi^0\Sigma^{*+}\bar{\Sigma}^{*-}, \Sigma^{*+} \to \pi^+\Lambda, \bar{\Sigma}^{*-} \to \pi^-\bar{\Lambda}, \Lambda \to \pi^- p,$ $\bar{\Lambda} \to \pi^+\bar{p}$	12	4
6	$\psi(3686) \to \eta\bar{\Sigma}^{*+}\Sigma^{*-}, \eta \to \gamma\gamma, \bar{\Sigma}^{*+} \to \pi^+\bar{\Lambda}, \Sigma^{*-} \to \pi^-\Lambda, \bar{\Lambda} \to \pi^+\bar{p},$ $\Lambda \to \pi^- p$	14	4
7	$\psi(3686) \to \pi^0\pi^0 J/\psi, J/\psi \to \pi^+\pi^-\Lambda\bar{\Lambda}, \Lambda \to \pi^- p, \bar{\Lambda} \to \pi^+\bar{p}$	4	3
others	Including 11 decay channels		14

连续本底的情况

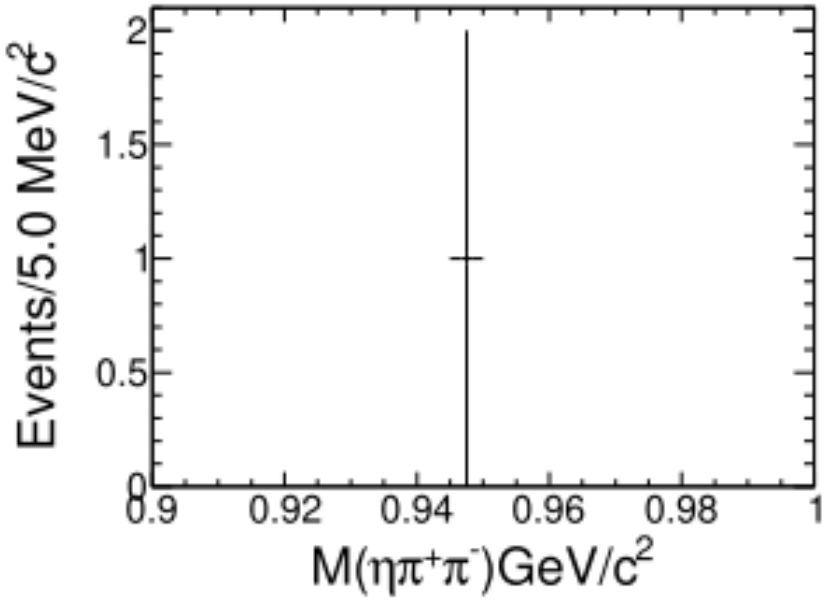

Figure 13: Invariant mass distribution of $\eta\pi^+\pi^-$ at center-of-mass energy of and 3.682 GeV/c^2 .

研究结果

信号事例数的获取

统计信号显著性为6.8σ (mode 1)

统计信号显著性为10σ (mode 2)

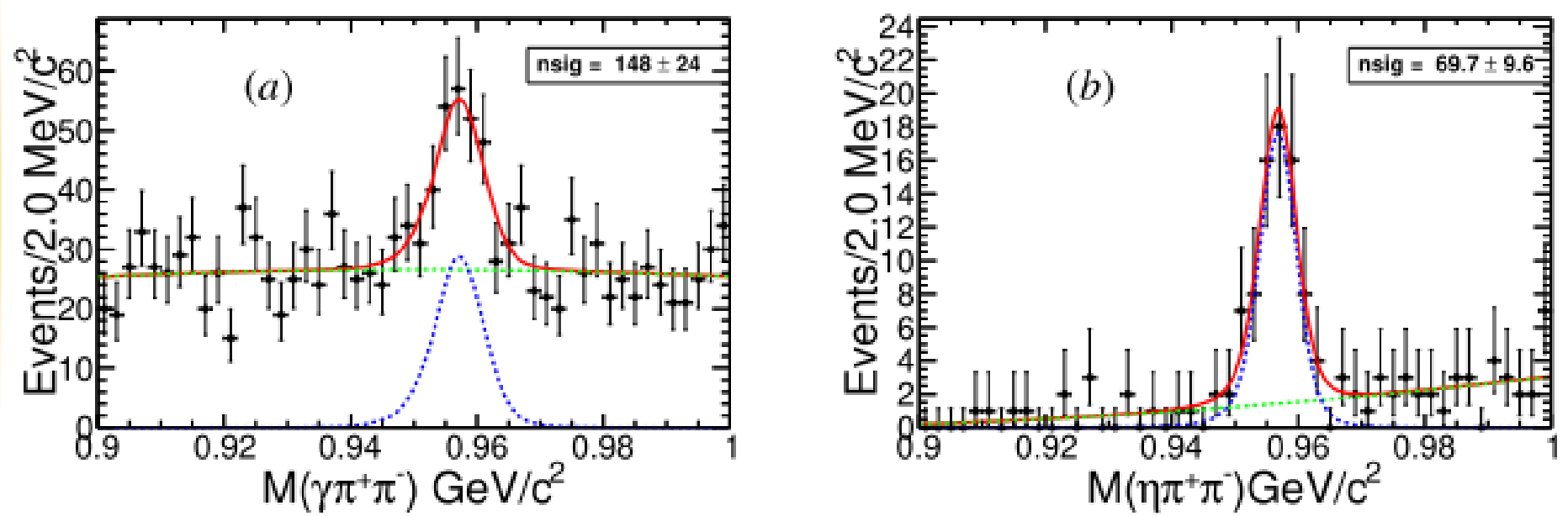

Figure 14: The fits to the mass spectra of M($\gamma\pi^+\pi^-$)(a) and M($\eta\pi^+\pi^-$)(b)

研究结果

分支比测量

Mode 1

$$\mathcal{B}(\psi(3686) \to \Lambda\bar{\Lambda}\eta', \eta' \to \gamma\pi^+\pi^-) = \frac{N^{obs}_{\gamma\pi\pi}}{N_{\psi(3686)} \times \mathcal{B}(\Lambda \to p\pi^-) \times \mathcal{B}(\bar{\Lambda} \to \bar{p}\pi^+) \times \mathcal{B}(\eta' \to \gamma\pi^+\pi^-) \times \epsilon_1}$$
$$= (6.97 \pm 1.13) \times 10^{-6}$$

Mode 2

$$\mathcal{B}(\psi(3686) \to \Lambda\bar{\Lambda}\eta', \eta' \to \eta\pi^+\pi^-)$$
$$= \frac{N^{obs}_{\eta\pi\pi}}{N_{\psi(3686)} \times \mathcal{B}(\Lambda \to p\pi^-) \times \mathcal{B}(\bar{\Lambda} \to \bar{p}\pi^+) \times \mathcal{B}(\eta' \to \eta\pi^+\pi^-) \times \mathcal{B}(\eta \to \gamma\gamma) \times \epsilon_2}$$
$$= (8.22 \pm 1.12) \times 10^{-6},$$

系统误差总结

Table 7: Systematic uncertainty for process $\eta' \to \gamma\pi^+\pi^-$

Source		Uncertainty(%)
$\psi(3686)$ total number*		0.7
MDC tracking*		6.0
PID efficiency*		6.0
Photon detection efficiency		1.0
Λ and $\bar{\Lambda}$ reconstruction efficiency*		2.0
Kinematic fit		0.55
Intermediate decays	$\Lambda \to p\pi^-$*	0.5
	$\bar{\Lambda} \to \bar{p}\pi^+$*	0.5
	$\eta' \to \gamma\pi^+\pi^-$	0.4
Mass window	$\Lambda(\pm 1 MeV/c^2)$	2.8
	$\bar{\Lambda}(\pm 1 MeV/c^2)$	1.9
	$J/\psi(\pm 2 MeV/c^2)$	0.8
	$\Sigma^0/\bar{\Sigma}^0(\pm 2 MeV/c^2)$	0.6
	$\chi_{c0}(\pm 3 MeV/c^2)$	1.5
	$\chi_{c1}(\pm 2 MeV/c^2)$	3.3
	$\chi_{c2}(\pm 2 MeV/c^2)$	3.8
	$\Xi^-/\bar{\Xi}^+(\pm 2 MeV/c^2)$	0.7
	$\Sigma(1385)(\pm 10 MeV/c^2)$	3.3
Fitting	Signal shape	0.7
	Background shape	2.0
	Fitting range	1.4
Total		11.7

Table 8: Systematic uncertainty for process $\eta' \to \eta\pi^+\pi^-$

Source		Uncertainty(%)
$\psi(3686)$ total number*		0.7
MDC tracking*		6.0
PID efficiency*		6.0
Photon detection efficiency		2.0
Λ and $\bar{\Lambda}$ reconstruction efficiency*		2.0
Kinematic fit		0.55
Intermediate decays	$\Lambda \to p\pi^-$*	0.5
	$\bar{\Lambda} \to \bar{p}\pi^+$*	0.5
	$\eta' \to \eta\pi^+\pi^-$	0.5
	$\eta \to \gamma\gamma$	0.18
Mass window	$\Lambda(\pm 1 MeV/c^2)$	1.7
	$\bar{\Lambda}(\pm 1 MeV/c^2)$	1.4
	$J/\psi(\pm 1 MeV/c^2)$	3.2
Fitting	Signal shape	0.7
	Background shape	1.2
	Fitting range	3.7
Total		10.6

总结

Table 9: Decay modes and branching fraction

Processes	Branching fraction
$\eta' \to \gamma\pi^+\pi^-$	$(6.97 \pm 1.13 \pm 0.82) \times 10^{-6}$
$\eta' \to \eta\pi^+\pi^-$	$(8.22 \pm 1.12 \pm 0.87) \times 10^{-6}$
Average	$(7.58 \pm 1.10) \times 10^{-6}$

展望

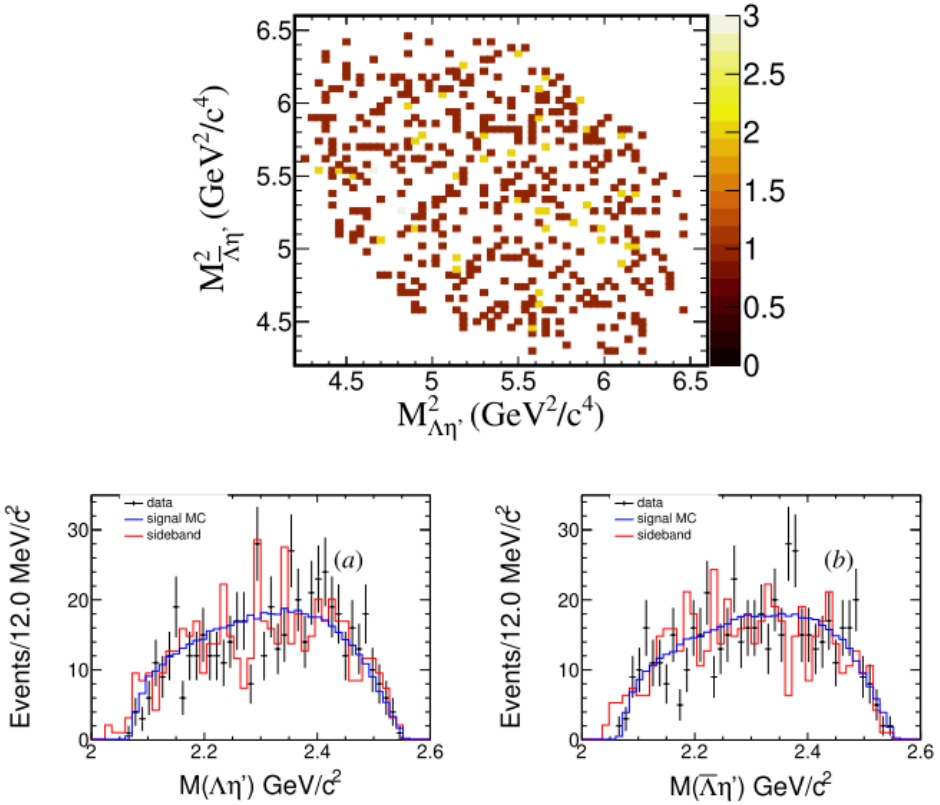

Figure 16: For Mode:$\eta' \to \gamma\pi^+\pi^-$, Dalitz plots of $M^2_{\Lambda\eta'}$ versus $M^2_{\bar{\Lambda}\eta'}$, and the mass distribution of $M_{\Lambda\eta'}$(a) and $M_{\bar{\Lambda}\eta'}$(b).

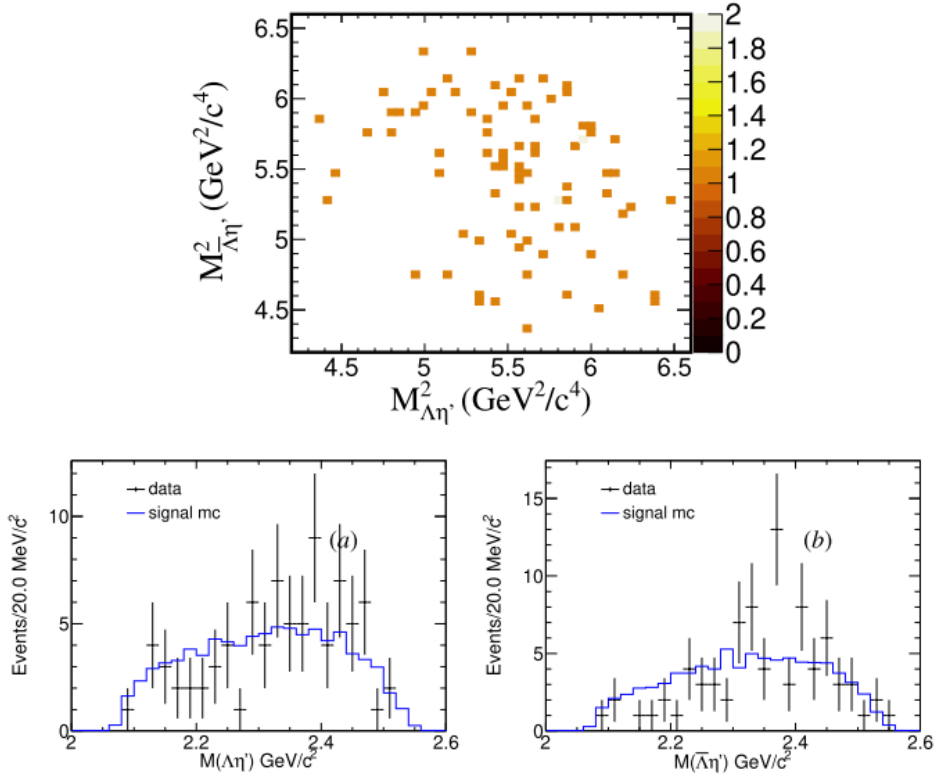

Figure 17: For Mode: $\eta' \to \eta\pi^+\pi^-$, Dalitz plots of $M^2_{\Lambda\eta'}$ versus $M^2_{\bar{\Lambda}\eta'}$, and the mass distribution of $M_{\Lambda\eta'}$(a) and $M_{\bar{\Lambda}\eta'}$(b).

谢谢大家！

恳请老师同学们的指正！

BUSINESS